TWO-STAGE AND THREE-STAGE VIRTUAL IMPACTOR SYSTEMS FOR BIOAEROSOL CONCENTRATION

A Thesis

by

JING WEN

Submitted to the Office of Graduate Studies of
Texas A&M University
in partial fulfillment of the requirements for the degree of

MASTER OF SCIENCE

December 2009

Major Subject: Mechanical Engineering

TWO-STAGE AND THREE-STAGE VIRTUAL IMPACTOR SYSTEMS FOR BIOAEROSOL CONCENTRATION

A Thesis

by

JING WEN

Submitted to the Office of Graduate Studies of
Texas A&M University
in partial fulfillment of the requirements for the degree of

MASTER OF SCIENCE

Approved by:

Co-Chairs of Advisory Committee,	Bing Guo
	Maria King
Committee Member,	Yassin A. Hassan
Head of Department,	Dennis L. O'Neal

December 2009

Major Subject: Mechanical Engineering

ABSTRACT

Two-Stage and Three-Stage Virtual Impactor Systems for Bioaerosol Concentration.

(December 2009)

Jing Wen, B.S., Xi'an Jiaotong University

Co-Chairs of Advisory Committee: Dr. Bing Guo
Dr. Maria King

The Circumferential Slot Virtual Impactor (CSVI) and The XMX/2A are two virtual impactors designed for sampling aerosol particles from a dilute environment by separating the aerosol into a fine and a coarse particle fraction. Dust particles in the ambient air may deposit within the virtual impactors and affect their performances. In this study the effect of dust loading within the CSVI on the efficiency of transmission was determined for particles from 0.49 to 9.9 μm in aerodynamic diameter (AD), and the performance of the three stage XMX/2A aerosol concentrator was characterized with 1 μm-9.9 μm AD polystyrene latex microspheres (PSL).

In the first experimental configuration, the two-stage CSVI had a first stage inflow of 100 L/min and a second stage minor flow of 1 L/min, each stage operating at an inflow/minor flow ratio of 10. An In-line Virtual Impactor (IVI) was used as a pre-separator for sampling inlets to exclude large particles. When the 100 L/min IVI with the two-stage CSVI was tested with Arizona Fine Road Dust (ARD A-2) particles, the transmission efficiency dropped to 50% when the dust entering the two-stage CSVI accumulated to about 100 mg. When it was tested with ASHRAE dust, a decrease of 43%

in the efficiency was detected after more than 200mg ASHRAE dust entered the two-stage CSVI. After cleaning the CSVI unit, the transmission efficiency returned to 99%, which indicated that the dust dissemination resulted in the plugging of the CSVI unit. The transmission efficiency of CSVI dropped more quickly below 50% when tested with the ARD A-2 dust, which had smaller particle sizes.

In the second configuration, XMX/2A, a three-stage aerosol concentrator designed to draw 800 L/min of air was used at a measured sampling flow rate of 742 L/min. XMX/2A equipped with an inlet was tested with 1 μm-9.9 μm AD PSL in a testing chamber. The peak transmission efficiency of XMX/2A was 39.5% for 8 μm AD PSL. By using the room air as cooling air and introducing dilution air to the flow cell, the transmission efficiency of each particle size increased.

A combination of monodisperse PSL and oleic acid particles represent the performance of CSVI. In the IVI-CSVI dust test, the CSVI unit SN003 had the best performance when tested with ASHRAE dust. XMX/2A had relatively low transmission efficiency when tested with PSL particles in the chamber.

ACKNOWLEDGEMENTS

I would like to thank my committee chairs, Dr. Bing Guo and Dr. Maria King, and my committee member Dr. Y. A. Hassan, for their seasoned guidance and help throughout my research.

I would also like to thank my beloved parents for their love and support.

NOMENCLATURE

C_c = Slip correction factor

D_p = Particle diameter

F_r = Fluorometer reading for a reference sample

F_s = Fluorometer reading for a sample collected downstream of a virtual impactor

L_c = Critical dimension; for circular jets L_c is the nozzle radius (*D/2*) for *Stk* and nozzle diameter (*D*) for *Re*, for slot jets L_c is the nozzle half-width (*W/2*) for *Stk* and the full-width (*W*) for *Re*

Q_r = Flow rate of the reference sample used in experimentation

Q_s = Flow rate into the virtual impactor

t_r = Duration of time a reference sample is collected

t_s = Duration of time a virtual impactor sample is collected

T = Transmission of aerosol particles of a given size through a virtual impactor. For a given particle size it is the ratio of aerosol particle mass flow rate at the minor flow exhaust port to aerosol particle flow rate at the inlet of the device.

U_o = Mean velocity at the exit of the accelerator section

V_s = Volume of the solvent used to elute tracer from an experimental sample

V_r = Volume of the solvent used to elute tracer from a reference sample

ρ_p = Particle density

ρ_f = Fluid density

μ_f = Dynamic viscosity of the fluid

TABLE OF CONTENTS

Page

CHAPTER Page

LIST OF TABLES

Page

LIST OF FIGURES

Page

Page

CHAPTER I

INTRODUCTION

1.1 Background

An aerosol concentrator would be subject to dust loading from the environment when deployed in the field. There are both military and civilian applications for such devices, such as the battlefields, the mining industry and the nuclear industry.

Virtual impactors are widely used for aerosol concentration. A virtual impactor is designed for sampling aerosol particles from a dilute environment by separating the aerosol into a fine and a coarse particle fraction (Seshadri et al., 2005). Figure B.1 shows the concept of the virtual impactor. The slot virtual impactor sharply redirects the majority airflow through an angle (typically 90°), allowing a small part of the airflow (about 10%) to proceed in the forward direction. Due to the high inertia of the large particles, they cannot take turns and thus proceed with the minor flow in the forward direction, while the major portion of the airflow and the smaller particles flow through the 90° angle. The larger particles in the minor flow are concentrated and the smaller particles in the minor flow pass through the system with little change in concentration.

This thesis follows the style and format of *Aerosol Science and Technology*.

In a circumferential slot virtual impactor (CSVI), the inlet aerosol enters on the circumference of the inlet blade, following a path radially inwards to the receiver impactor blades (Haglund and McFarland 2004). The two-stage CSVI (TSI Inc., Shoreview, MN), as shown in Figure B.2a, has two virtual impactors operated in series. For the first stage of the CSVI, the entrance flow rate is 100 L/min and the flow rate of the exhaust air is 10 L/min. With the same ratio of major to minor flow, the second stage CSVI, using the first stage exhaust stream as the entrance flow, has a minor flow rate of 1 L/min. If the virtual impactor is 100% efficient for a given particle size, the 1 L/min minor flow will contain the same number of large aerosol particles as present in the original 100 L/min flow.

When a virtual impactor is used in an environment where there is a large amount of unwanted very large particles (e.g., >10 μm), a pre-separator may be needed to scalp large particles from the aerosol size distribution. An in-line virtual impactor (IVI, TSI Inc., Shoreview, MN) shown in Figure B.3 is designed as a pre-separator for sampling inlets to exclude large particles (Seshadri 2007). The schematic of the IVI is shown in Figure B.4. The major flow rate of IVI is 100 L/min, which can be used as the entrance flow of the CSVI.

Dust particles, especially fibrous particles (e.g. lint), will deposit on the critical surfaces within the CSVI and hence may affect the penetration of the target aerosol particles. Periodic maintenance will be needed to clean the CSVI to restore the

performance. Understanding the effect of dust loading on the performance of the CSVI is vital for making maintenance decisions.

Multistage aerosol concentrator with high-volume flow rate is widely used in many situations, such as detection of biological aerosols at low concentration, laboratory aerosol sampling, clean room monitoring, and ambient aerosol measurements (Kim et al., 2001). Multistage aerosol concentrator can improve the performance of aerosol concentration. XMX/2A (Figure B.5a-B.5d, Dycor Technologies Ltd., Alberta, Canada) is a three-stage aerosol concentrator with three virtual impactors operated in a series. The designed total inlet flow rate of the XMX/2A is 800 L/min, while the minor flow rate of the third stage is set at 1 L/min.

1.2 Literature Review

The first impactor, named a éroscope, was developed by M. F. Pouchet in 1860 for inhalation studies and air sampling in hospitals, swamplands and mountains (Marple 2004). It was used for quickly collecting particles and examining them under a microscope to obtain the correlation between the ambient air and the disease affecting the patients. Until the 1960's, the impactors were developed as a jet of particle-laden air impinging on a plate, which were called 'Real or Classical Impactors'.

Hounam and Sherwood (1965) designed a virtual impactor to solve the particles impaction plate problems. By replacing the real impactor surface in an inertial impactor with a virtual collection surface, the virtual impactor eliminated problems associated with

the interaction of the particles with the impaction surface, such as fragmentation, bounce, overload, and reentrainment.

Both experimental and theoretical studies were conducted on the two-dimensional slit virtual impactors (Ravenhall et al. 1978, 1982; Forney et al. 1982). Ravenhall et al. (1978) presented the particle sizing capabilities of virtual impactors such as efficiency curve steepness and properties of the internal loss spectrum. Ravenhall et al. (1982) theoretically predicted the characteristics of a two-dimensional slit virtual impactor using potential flow analysis and solutions to Navier-Stokes equations. Numerical computation showed that the internal particle losses reduce to zero as the normalized void width increased to $h/w = 1.4 \pm 0.1$, where w is the width of the throat and h is the perpendicular opening. The steepness of the particle efficiency curves was reduced by increasing the void width. Forney et al. (1982) experimentally investigated the influence of geometry on the impactor performance, which matched well with the theoretical models. By using tracer dye in a scaled-up water model to study the properties of the flow field, Forney et al. (1982) also found out that the acceleration nozzle Reynolds numbers should be in the range of $700 < Re < 1600$ to maintain a stable flow field behavior.

Chen et al. (1985) certified that a virtual impactor can be used as size-selective sampler and investigated the influence of nozzle Reynolds number as well as the minor-to-total flow ratio in a virtual impactor nozzle. Experimental results showed that the

separation efficiency curves were influenced by the ratio of minor flow rate to the total flow rate, but not affected by the nozzle Reynolds number.

A modified virtual impactor with a clean air core in the center of an aerosol flow has been studied (Masuda et al. 1979; Chen et al. 1986). With a clean air core introduced at the acceleration nozzle inlet, the virtual impactor could eliminate the fine particle contamination in the coarse particle stream, and improve the particle separation characteristics. However, the disadvantage of such prototype impactor was the internal wall losses.

Loo and Cork (1988) conducted an experimental study with a single stage virtual impactor. The results showed that the nozzle wall losses increase 1% with each 0.05 mm increase in nozzle misalignment. They stated two principles which are critical to the impactor performance. The first one is that the internal physical surfaces should match the streamlines accordingly based on theoretical description of the flow field and the knowledge of impaction theory. The second one is the importance of symmetry.

Hassan et al. (1978) and Marple and Chien (1980) conducted analytical studies on round virtual impactors. Hassan et al. (1978) assumed that the particle presence did not affect the flow field in the analytical model and got good agreement between the model and experimental results. Marple and Chien (1980) characterized the virtual impactors by using the numerical solution of the Navier-Stokes equations and of the equations of motion of the particles. The results showed that significant losses on the inner surface of

the collection probe were found at the cutoff particle size. Most geometry parameters had little influence on the large particle collection efficiency, while they had significant effect on the small particle collection efficiency.

Haglund and McFarland (2004) first designed and conducted experiments on a circumferential slot virtual impactor (CSVI). Hari (2003) modeled the CSVI and his simulation results matched with Haglund's experimental results very well. Hu et al. (2009) modified the CSVI units by placing a cone upstream of the second stage of a two-stage CSVI, and introducing sheath air to displace the stagnation region away from the cone. Experimental results had good agreement with Computational Fluid Dynamics analysis, showing that the transmission efficiency of the CSVI increased from 4% to 90% by applying 1.8% of inlet flow rate sheath air to the cone.

Multistage virtual impactors were designed for bioaerosol concentration with two or more virtual impactors in a series, sampling aerosol particles at high volume flow rate. Kesavan et al. (2008) characterized five multistage concentrators, including XMX/2A aerosol concentrator, with five nonviable and viable laboratory aerosols. The test results showed that for large particle sizes (> 6 μm AD), liquid and dry particles had different efficiencies. Kim et al. (2001) designed and fabricated a two-stage aerosol concentrator with a total inlet flow rate of 1000 L/min. The aerosol concentrator was calibrated using polystyrene latex particles in aerodynamic sizes ranging from 0.5 to 10 μm. The aerosol concentration performance was significantly improved with multistage aerosol

concentrator.

1.3 Objective of the Present Study

The objective of this study is to characterize the transmission efficiency of the two-stage CSVI units and XMX/2A for particle sizes ranging from 0.49 to 10 μm AD at a fixed volumetric flow rate, and determine the effect of dust loading within the two-stage CSVI on the efficiency of penetration for particles from 0.49 to 10 μm in aerodynamic diameter.

CHAPTER II

THEORY

The performance of a virtual impactor is characterized by two dimensionless parameters, the Stokes number (*Stk)* and the Reynolds numbers (*Re*):

$$Stk_{Lc} = \frac{\rho_p \cdot D_p^{\,2} \cdot C_c \cdot U_o}{18 \cdot \mu_f \cdot L_c} \qquad [1]$$

$$\mathrm{Re}_{Lc} = \frac{\rho_f \cdot U_o \cdot L_c}{\mu_f} \qquad [2]$$

where:

C_c = slip correction factor

D_p = particle diameter

L_c = critical dimension; for circular jets L_c is the nozzle radius (*D/2*) for *Stk* and nozzle diameter (*D*) for *Re*, for slot jets L_c is the nozzle half-width (*W/2*) for *Stk* and the full-width (*W*) for *Re*

U_o = mean velocity at the exit of the accelerator section

ρ_p = particle density

ρ_f = fluid density

μ_f = dynamic viscosity of the fluid

The Stokes number for a virtual impactor is defined as the ratio of the particle stopping distance at the average nozzle exit velocity to half the jet width, which is the dominant parameter governing the behavior of particles in the virtual impactor.

The Reynolds number is the ratio of inertial forces to viscous forces in the air flow. For the first and second stages of CSVI in this study, the Reynolds number were 994 and 235 based on the slot widths and nominal intake flow rates (LaCroix 2008), which can be considered as the laminar flow.

The performance of a virtual impactor is based on the rate at which particles were exhausted in the minor flow compared to the rate of aerosol particle entering the system. The transmission efficiency is calculated as below:

$$T = \frac{\frac{F_s V_s}{Q_s t_s}}{\frac{F_r V_r}{Q_r t_r}} \qquad [3]$$

where:

t_r = Duration of time a reference sample is collected

t_s = Duration of time a virtual impactor sample is collected

T = Transmission of aerosol particles of a given size through a virtual impactor.

For a given particle size it is the ratio of aerosol particle mass flow rate at the minor flow exhaust port to aerosol particle flow rate at the inlet of the device.

V_s = Volume of the solvent used to elute tracer from an experimental sample

V_r = Volume of the solvent used to elute tracer from a reference sample

Q_r = Flow rate of the reference sample used in experimentation

Q_s = Flow rate into the virtual impactor

F_r = Fluorometer reading for a reference sample

F_s = Fluorometer reading for a sample collected downstream of a virtual impactor

In this study, the volume of solvent used to elute tracer from a reference sample (V_r) and an experimental sample (V_s) were the same. Also, the duration time for reference and experimental sample were the same. Equation 4 was used to evaluate performance of virtual impactors.

$$T = \frac{F_s Q_r}{F_r Q_s} \qquad [4]$$

CHAPTER III

EXPERIMENTAL METHODOLOGY

In this study, two virtual impactors, CSVI and XMX/2A, were tested with monodisperse PSL, oleic acid particles and test dust at a fixed volumetric flow rate. The transmission efficiency of the virtual impactor is dependent on the air flow rate and the particle size. Room temperature and the relative humidity of the ambient will also affect the performance of the virtual impactors.

3.1 Different Types of Virtual Impactors

3.1.1 Two-Stage Circumferential Slot Virtual Impactor (CSVI)

A two-stage CSVI manufactured at TSI Inc., (Burnsville, MN) shown in Figure B.2a is designed for sampling aerosol particles from a dilute environment by separating the aerosol into a fine and a coarse particle fraction. In the CSVI, the inlet aerosol enters on the circumference of the inlet blade, following a path radially inwards to the receiver impactor blades (Haglund and McFarland 2004). The two-stage system equipped with an automatic flow system (AMETEK, Paoli, PA) has two virtual impactors operated in series. For the first stage (Figure B.2b), the entrance flow rate is 100 L/min and the flow rate of the exhaust air is 10 L/min. With the same ratio of major to minor flow, the second stage (Figure B.2c), using the first stage exhaust stream as the entrance flow, has a minor flow rate of 1 L/min. If the virtual impactor is 100% efficient for a given particle

size, the 1 L/min minor flow will contain the same number of large aerosol particles as present in the original 100 L/min flow.

The inner diameter of the first stage plenum is 127 mm. The first stage acceleration nozzle has a width of 0.711 mm. The cusp on the top part of the first stage is used to direct aerosol particles to the minor flow exhaust tube (LaCroix 2008). The second stage plenum chamber has a diameter of 76 mm. The overall height of the second stage unit is 76.2 mm, while the acceleration nozzle width is 0.35 mm. On top of the second stage CSVI, a cone with a height of 30.5 mm was placed to uniformly distribute aerosol particles, thus, the second stage inlet could get uniform aspiration aerosols (Hu et al. 2009). Sheath air is exhausted at a low flow rate from the apex of the cone to reduce the particle losses. Both numerical simulations and experiments were conducted by Hu et al. (2009). The results showed that the transmission efficiency was increased by 86% when the sheath air cone was applied for 10 μm particles tested with a 100 L/min two-stage CSVI.

3.1.2 In-line Virtual Impactor (IVI)

A Dual-Cone In-line Circumferential Slot Virtual Impactor (IVI) is designed as a pre-separator for sampling inlets to exclude large particles >10 μm (Seshadri et al. 2008). The schematic of the IVI is shown in Figure B.4. Aerosol particles enter the IVI split in two parts, the major flow and the minor flow. The major flow including 90% of the total flow contains fine particles, which can be used as the entrance flow of the CSVI. The

major flow rate of IVI is 100 L/min with a cutpoint size of 10 μm AD, which defines as the smaller aerodynamic particle diameter at which transmission equals 50%. The minor flow, which comprises 10% of the total flow, has a flow rate of 11 L/min. The lower cone has an apex angle of 90° to reduce the recirculation zones in the major flow area and ensure flow stability (Seshadri et al. 2008).

3.1.3 XMX/2A Virtual Impactor

Multistage virtual impactors, which operate virtual impactors in series, will have higher aerosol concentration than a single stage impactor. The XMX/2A is a three-stage aerosol concentrator designed to pull 800 L/min of air, while the measured sampling flow rate is 742 L/min (Kesavan et al. 2008). The three-stage virtual impactor was tested in a 25” by 24” by 24” chamber, with a cap on the top of the inlet to prevent droplets (rain) from entering the XMX. The minor flow rate of the third stage is 1 L/min.

3.2 Test Procedures

3.2.1 Testing the CSVI with Monodisperse Polystyrene Latex Fluorescent Aerosol Particles

In this study, solid monodisperse Polystyrene Latex (PSL) microspheres (Nanosphere Size Standards, Duke Scientific, Palo Alto, CA) between 0.49-9.9 μm were used to characterize the transmission efficiency in the major and minor flow of the two-stage circumferential slot virtual impactor. The test setup consisting of the impactor and a 7 ft long, 6” diameter flow cell is shown on Figure B.6.

The CSVI units equipped with an automated flow system were first tested with different sizes of PSL. PSL particles were aerosolized by a six-jet Collison nebulizer (Model CN 311, BGI Inc., Waltham, MA) at 138 kPa (20 psi), and were collected on 47mm A/D glass fiber filters (Pall Corp., Ann Arbor, MI) attached to minor flow (1 L/min) of the CSVI units during 10min aerosolization periods. As a reference, a 4"A/E glass fiber filter (HI-Q, San Diego, CA) was used to replace the CSVI and collected PSL at 100L/min for the same period of time. The filters were soaked in 15ml of ethyl acetate to dissolve the fluorescent dye and analyzed by the Quantech fluorometer (Model 109535, Barnstead International, Dubuque, IA) fitted with a narrow band NB 540 nm optical excitation filter and a narrow band NB 590 nm filter as the optical emission filter for red PSL, and a narrow band NB 460 nm optical excitation filter and a narrow band NB 490 nm filter as the optical emission filter for green PSL, respectively. The FIU (Fluorescent Intensity Unit) values were compared to the values of the reference filters collected at 100 L/min for the same periods of time.

3.2.2 Testing the CSVI with Monodisperse Liquid Fluorescent Aerosol Particles

The CSVI units were also tested with monodisperse liquid aerosols using a different setup (Figure B.7). Oleic acid particles containing sodium fluorescein were generated by the VOAG (Vibrating Orifice Aerosol Generator, TSI, Shoreview, MN), for 30sec aerosolization and collection periods. The particle sizes were analyzed by the APS (Aerodynamic Particle Sizer, TSI, Shoreview, MN) and also by microscope, at 40x

magnification using a 10x additional eyepiece. During testing, the particles were captured on 47mm glass fiber filters and dissolved in 30ml of 50% isopropanol at pH 9.0. The FIU values were analyzed at NB490/SC515 and compared to the reference filter values.

3.2.3 Testing the CSVI with Dust Particles

To determine the amount of dust that can enter the CSVI without affecting its performance, the 100 L/min IVI with the Two-Stage CSVI was tested with the mineral-carbon-fibre ASHRAE (The American Society of Heating, Refrigerating and Air-Conditioning Engineers) test dust (72% Arizona Road Dust A-2, 23% Morocco Black and 5% cotton lint) and Arizona Fine Road Dust (ISO 12103–1, A2 Fine test Dust, Powder Technology Inc., MN) and 5 μm polystyrene latex beads. The IVI was operated at 100 L/min and 100 L/min total intake flow was directed into the CSVI. The test setup containing a six-jet Collison nebulizer for the aerosolization of the PSL at 138 kPa (20 psi) and a fluidizing bed for the dissemination of the dust (mixture of 100g of 0.1mm zirconia/silica beads and 5g of test dust) at 207 kPa (30 psi) is shown on Figure B.8. The dust was disseminated through a Kr-85 neutralizing source (TSI, Shoreview, MN) for a period of time (60 min), scalped by the IVI and concentrated by the two-stage CSVI at 100 L/min. The particles carried by the IVI major flow and the CSVI minor flow were captured on 47mm A/D glass fiber filters, to measure the amount of dust exiting the CSVI. As a reference, a 4” A/E glass fiber filter was used to replace the CSVI and collect dust at 100 L/min for the same period of time, which indicated the amount of dust

entering CSVI. Each cycle of 60 min periods of dust dissemination for the reference filter and CSVI, respectively, was followed by 5 min periods aerosolizing PSL particles into the reference filter and the CSVI without prior cleaning of the concentrator. The effect of dust loading on the performance of CSVI was evaluated by the relationship between the amount of dust entering CSVI and the PSL transmission efficiency.

The filters were weighed before and after collection on a Mettler AB104 balance to 0.0001g. The deposition of the dust particles on the filters was analyzed by the Multisizer 3 Coulter Counter (Beckman Coulter Inc., Fullerton, CA), using the 100 μm orifice. The amount of PSL collect on the filters was dissolved in 15 ml of ethyl acetate and analyzed by a fluorometer fitted with a narrow band NB 540 nm optical excitation filter and a narrow band NB 590 nm filter as the optical emission filter. The tests were continued for several cycles with increasing amounts of dust accumulating in the CSVI.

3.2.4 Testing the XMX/2A with Monodisperse Polystyrene Latex Fluorescent Aerosol Particles

In the setup the XMX/2A equipped with the inlet was placed in a 25” x 24” x 24”chamber, to achieve a uniform aerosol concentration. A 6-jet Collison nebulizer was used for the aerosolization of the PSL suspension at 138 kPa (20 psi) for 10 min, using a fresh 30 mL batch for each sample. The aerosolized particles were introduced through a 7 ft long horizontal 6” pipe, with a 3 ft long 6” vertical section turned downwards to connect to the chamber. Room air was used to cool the XMX/2A through a 2.5” pipe.

Dilution air was introduced to the horizontal flow cell through a 1” plastic tube, allowing the aerosolized PSL particles to dry in the flow cell. The particles carried by the minor flow at 1 L/min were captured on 47mm A/D glass fiber filters. As a reference, a 4”A/E glass fiber filter was placed in the chamber and operated simultaneously with the aerosol concentrator at 100 L/min. The test setup with and without dilution air are shown in Figure B. 9 and B.10, respectively.

CHAPTER IV

RESULTS AND DISCUSSION

4.1 Two-Stage Circumferential Slot Virtual Impactor (CSVI)

4.1.1 Transmission Efficiency of the 100 L/min Two-Stage CSVI Units: TSI SN001-003 Using Polystyrene Latex Particles and Monodisperse Liquid Particles

Liquid and polystyrene latex fluorescent monodisperse particle tests were conducted on three two-stage 100 L/min CSVI units (SN001-003). The transmission efficiency of the three CSVI units is shown in Table A.1 and Figure B.11. The cutpoint particle size was 2.5 μm AD. The transmission efficiency was about 0.05% at a particle size of 0.49 μm AD and increased with particle size. The peak transmission efficiency was about 100% for the 7.2 μm AD particle size. The transmission efficiency decreased to 80% when the particle size increased to 9.9 μm AD.

4.1.2 PSL Transmission Efficiency of the IVI-CSVI in the Presence of Increasing Amounts of Test Dust

100 L/min IVI with a new 100 L/min two-stage CSVI unit SN003 was tested with the mineral-carbon-fibre ASHRAE test dust and 5 μm PSL. As shown in Table A.2 and Figure B.12a, the PSL transmission efficiency dropped below 50% when the dust entering CSVI accumulated to about 200 mg. Figure B.12b shows the ASHRAE dust deposition in the CSVI after the experiment.

IVI with four 100 L/min Two - Stage CSVI units (SN003-006) were tested with Arizona Fine Road Dust (ARD A-2) and 5 μm polystyrene latex beads. Table A.3 and Figure B.13a show the PSL transmission efficiency of the IVI-CSVI SN003-006 in the presence of unevenly increasing amounts of ARD A-2 dust. Before the dust test, the initial transmission efficiency of 5μm PSL was about 94%. For CSVI units SN003-006, the transmission efficiency dropped below 50% when the dust entering CSVI accumulated to about 95 mg, 67 mg, 95 mg and 56 mg, respectively. The ARD A-2 dust deposition in the CSVI SN003 is shown in Figure B.13b. After cleaning the CSVI units, the transmission efficiency returned to 99%, which indicated that the dust dissemination resulted in the plugging of the CSVI units.

Compared with the ASHRAE dust test, the PSL transmission efficiency dropped below 50% when a smaller amount of ARD A-2 dust was disseminated into the CSVI unit, which indicates that the ARD A-2 fine dust with a smaller particle sizes plug the CSVI units easier than the ASHRAE dust. The test results also show that with a new CSVI unit, the performance of CSVI is better than the units used for testing, indicating that the decrease in the performance may be due to the dust deposition inside the automatic flow system.

4.2 XMX/2A Aerosol Concentrator

4.2.1 Transmission Efficiency of XMX/2A Test with PSL with Dilution Air

XMX/2A equipped with the inlet was placed in a 34" x 24" x 24"chamber tested with different sizes of PSL with additional air drying the PSL particles. The dilution air was used to remove any moisture on the aerosol particles and also to achieve appropriate humidity at the sampling point. Table A.4 and Figure B.14 show the PSL transmission efficiency of XMX/2A with 1μm-9.9 μm AD PSL particles. The peak transmission efficiency was 39.5% which occurs at 8μm AD.

4.2.2 Transmission Efficiency of XMX/2A Test with PSL without Dilution Air

Table A.5 and Figure B.15 shows the PSL transmission efficiency of XMX/2A tested without additional dilution air. The transmission efficiency curve had an inverted 'U' shape, which had lower efficiencies for very small and very large particles. The low efficiency of small particles was due to cutpoint considerations of the fractionators and the efficiency of larger particles was reduced by internal losses of aerosol particles (Kesavan et al., 2008). The peak transmission efficiency was 29% at a particle size of 5μm AD, which was lower than the transmission efficiency of XMX/2A tested with dilution air. This result might be caused by introducing dilution air to the test setup, which could make the particles in the flow cell drier. Wet particles may deposit inside the XMX/2A and cause low transmission efficiency.

4.2.3 Discussion of the Problems Associated with the XMX Testing

The performance of XMX/2A was found to be unstable, resulting in relatively low transmission efficiency. For the three replicates of each test, the transmission efficiency of the last one or two replicates dropped below 1%. After cleaning up the three stages of XMX/2A, the transmission efficiency returned to around 30%.

Figure B.16 shows the Borescope images of discolored/damaged areas inside the XMX/2A second stage ¼" nozzle at the connection to the $^{1}/_{20}$" section, where particles may settle down.

Relative humidity of the testing chamber was also evaluated for 30 minutes during the test. As shown in Figure B.17, the temperature in the chamber increased from 74° F to 84° F, while the relative humidity decreased dramatically after 30 minutes, which indicated that the environment in the chamber was dry.

Room air was introduced to the XMX/2A as cooling air by a 2.5" pipe. The transmission efficiency of 5μm AD PSL increased by 1.6 times as the PSL transmission efficiency without the cooling air.

4.3 Uncertainty Analysis

The uncertainties of the various parameters were determined from manufacturer reported data, from observations of repeatability of measured quantities, or from reasonable assumptions of error when no data was available. The uncertainty values in the flowmeter measurement were determined based on the taken from manufacturer's

manual as well as on the precision errors resulting from reading the flowmeter. The uncertainty in the CSVI second stage nozzle length and width were also taken from the manufacturer. The uncertainty of testing time is determined by the precision of the timing device and reading. The precision error of the fluorescent intensity readings is taken from the average variance of replicate readings of the same sample. The non-constant dust generation rate causes precision error. And the measurement of the filters' weight is also a source of uncertainty.

Kline and McClintock (1953) presented a method of estimation uncertainty in experimental results. The equation used to calculate uncertainty is shown below:

$$w_R = \left[\sum_{i=1}^{n} \left(\frac{\partial R}{\partial x_i} \delta w_i \right)^2 \right]^{\frac{1}{2}} \qquad [5]$$

The result R is a given function of the independent variables x_i. w_R is the uncertainty in the result and w_i are the uncertainties in the independent variables.

Transmission efficiency is calculated by equation 4 with the assumption that the sample times and the volume of the solutions are the same. Applying equation 5, the uncertainty of transmission efficiency calculation is:

$$w_T = \left[\left(\frac{\partial T}{\partial F_s} w_{F_s} \right)^2 + \left(\frac{\partial T}{\partial Q_r} w_{Q_r} \right)^2 + \left(\frac{\partial T}{\partial F_r} w_{F_r} \right)^2 + \left(\frac{\partial T}{\partial Q_s} w_{Q_s} \right)^2 \right]^{\frac{1}{2}} \qquad [6]$$

The relative uncertainties of Q_r and Q_s are both 2.5% (LaCroix 2008). So as shown in equation 7, the relative uncertainty of transmission efficiency is a function of the reference and sample fluorometer readings.

$$\frac{w_T}{T} = \left[(0.025)^2 + (0.025)^2 + \left(\frac{\delta F_s}{F_s} \right)^2 + \left(\frac{\delta F_r}{F_r} \right)^2 \right]^{\frac{1}{2}} \quad [7]$$

where δF_r is the uncertainty value of the fluorometer reading of a reference sample and δF_s is the uncertainty value of the fluorometer reading of a CSVI sample. For each test, t hree replicate samples were taken consecutively under the same operating conditions, whi ch may not produce the same fluorescence values due to random errors. The minimum an d maximum errors are $\pm 3.2\%$ and $\pm 13.1\%$.

CHAPTER V

SUMMARY AND CONCLUSION

A 100 L/min two-stage circumferential slot virtual impactor was tested with liquid and Polystyrene Latex Fluorescent monodisperse aerosols. The two-stage CSVI had a cutpoint Stokes number of 1.2 and a cutpoint particle size of 2.5 μm AD. The maximum transmission efficiency was 100% for the particle size of 7.2 μm AD.

When the 100 L/min IVI with the two-stage CSVI tested with ARD A-2 dust, the transmission efficiency dropped to 50% when the dust entering the two-stage CSVI accumulated to about 100 mg. When tested with ASHRAE dust, a decrease in the efficiency was detected after more than 200mg ASHRAE dust entered the two-stage CSVI. After cleaning up the CSVI and the automatic flow system, the transmission efficiency returned to 99%, which indicated that the dust dissemination resulted in the plugging of the CSVI unit. The CSVI performed better when tested with the ASHRAE dust, which has bigger dust particle sizes.

A three-stage aerosol concentrator XMX/2A was tested with 1-9.9 μm AD PSL in a testing chamber. The peak transmission efficiency of XMX/2A was 39.5% for 8 μm AD PSL. By using the room air as cooling air and introducing dilution air to the flow cell, the transmission efficiency of each particle size increased.

REFERENCES

Chen, B. T., Yeh, H. C., and Cheng, Y. S. (1985). A Novel Virtual Impactor: Calibration and Use. *J. Aerosol Sci.*, 16:343-354.

Chen, B. T., Yeh, H. C., and Cheng, Y. S. (1986). Performance of a Modified Virtual Impactor. *Aerosol Sci. Technol,* 5:369-376.

Forney, L.J., Ravenhall, D.G., and Lee, S.S. (1982). Experimental and Theoretical Study of a Two-Dimensional Virtual Impactor. *Environ. Sci. & Technol,* 16:492-497.

Haglund, J. S. and McFarland, A. R. (2004). A Circumferential Slot Virtual Impactor. *Aerosol Sci. Technol*, 38:664-674.

Hari, S. (2003). Computational Fluid Dynamics (CFD) Simulations of Dilute Fluid-Particle Flows, Ph.D. Dissertation, Department of Nuclear Engineering, Texas A&M University, College Station, TX.

Hassan, Y. A., Jones, B. G., and Yule, T. J. (1978). An Analytical Study of Virtual Impactor Aerosol Separators. *Transactions of the American Nuclear Society*, 33:182-184.

Hounam, R. F. and Sherwood, R. J. (1965). The Cascade Centripeter: A Device for Determining the Concentration and Size Distribution of Aerosols. *Amer. Ind. Hyg. Assoc. J.*, 26:122-131

Hu, S., LaCroix, D. E., and McFarland, A. R. (2009). Stagnation Point Displacement: Control of Losses on a Conically Shaped Aerosol Distributor. *Aerosol Sci. Technol,* 43:311-321.

Kesavan, J., Bottiger, J. R., and McFarland, A. R. (2008). Bioaerosol Concentrator Performance: Comparative Tests with Viable and with Solid and Liquid Nonviable Particles. *Journal of Applied Microbiology*, 104:285–295.

Kim, M. C., Kim, D. S., Lee, K. W., Youn, H. J., Choi, K. B., and Ha, Y. C. (2001). Multijet and Multistage Aerosol Concentrator: Design and Performance Analysis. *Journal of Aerosol Medicine*, 14:245-254.

Kline, S. J., and McClintock, F.A. (1953). Describing Uncertainties in Single-Sample Experiments, *Mech. Eng.* 73:3-8.

LaCroix, D. E. (2008). A Two-Stage 100 L/min Slot Virtual Impactor System for Bioaerosol Concentration, M.S. Thesis, Department of Mechanical Engineering, Texas A&M University, College Station, TX.

Loo, B. W., and Cork, C. P. (1988). Development of High Efficiency Virtual Impactors. *Aerosol Sci. Technol*, 9:167-176.

Marple, V. A., and Chien, C. M. (1980). Virtual Impactors: A Theoretical Study. *Environ. Sci. Technol,* 14:976-985.

Marple, V. A. (2004). History of Impactors - The First 110 Years. *Aerosol Sci. Technol*, 38:247-292.

Masuda, H., Hochrainer, D., and Stober, W. (1979). An Improved Virtual Impactor for Particle Classification and Generation of Test Aerosols with Narrow Size Distributions. *J. Aerosol Sci.* 10:275-287.

Ravenhall, D. G., Forney, L. J., and Jazayeri, M. (1978). Aerosol Sizing with a Slotted Virtual Impactor. *Journal of Colloid and Interface Science*, 65:108-117.

Ravenhall, D. G., Forney, L. J., and Hubbard, A. L. (1982). Theory and Observation of a Two-Dimensional Virtual Impactor. *Journal of Colloid and Interface Science*, 85:508-520.

Seshadri, S., Phares, D. J., Kim, T., Kihm, K. D., Smith, D. D., and McIntyre, P. M. (2005). Performance of a Slit Virtual Impactor Operated at High Particle Mass Loading. *J. Aerosol Sci.*, 36:541-547.

Seshadri, S. (2007). The In-Line Virtual Impactor, Ph.D. Dissertation, Department of Mechanical Engineering, Texas A&M University, College Station, TX.

Seshadri, S., Hari, S., Hu, S., and McFarland A. R. (2008). A Circumferential Slot In-Line Virtual Impactor. *Aerosol Sci. Technol.*, 42:40-49.

APPENDIX A

TABLES

Table A.1 Transmission efficiency of the three two-stage CSVI 100 L/min units using particles 0.49 μm - 9.9 μm

Particle	Size (μm)	CSVI SN001 Transmission Efficiency (%)	CSVI SN002 Transmission Efficiency (%)	CSVI SN003 Transmission Efficiency (%)
PSL (red)	0.49	5	4	5
PSL (green)	1.5	7	6	6
PSL (red)	2	18		
Oleic acid	2.5	49		49
PSL (red)	3	71	79	78
PSL (green)	5	95	95	92
Oleic acid	5.7	95	90	90
Oleic acid	7.2	100	101	98
Oleic acid	8	87	91	92
PSL (green)	9.9	81	79	82

Table A.2 PSL (5 μm) transmission efficiency of a two-stage 100 L/min CSVI (TSI SN/003) in the presence of increasing amount of ASHRAE dust accumulation

Dust Dissemination Period	ASHRAE Dust Into CSVI (mg)	PSL Transmission Efficiency (%)
0	0	94
1	5.4	93
2	15.6	92
3	30.5	90
4	49.0	92
5	66.9	90
6	97.6	84
7	118.9	86
8	146.9	88
9	173.2	81
10	204.6	82
11	222.5	17

Table A.3 PSL transmission efficiency of the IVI-CSVI SN003-006 in the presence of increasing amounts of ARD A-2 dust

	CSVI SN003		CSVI SN004		CSVI SN005		CSVI SN006	
Test Period	Dust Into CSVI (mg)	PSL Eff.(%)	Dust Into CSVI (mg)	PSL Eff.(%)	Dust Into CSVI (mg)	PSL Eff.(%)	Dust Into CSVI (mg)	PSL Eff. (%)
0	0	94	0	95	0	98	0	95
1	37.5	91	16.3	92	18.9	72	5.9	79
2	49.7	88	20.7	82	39.9	76	19.7	67
3	57.6	91	29.7	76	86.3	57	35.8	57
4	65.7	87	38.2	76	95.0	34	55.9	32
5	72.7	67	47.6	78				
6	79.4	73	53.9	63				
7	85.3	61	61	59				
8	95.1	47	67.3	46				
9	99.8	35						

Table A.4 PSL transmission efficiency of XMX/2A using 1 μm-9.9 μm AD PSL particles with dilution air

Particle Size(μm)	Transmission Efficiency(%)
1	1.6
2	3.6
3	16.7
4.8	37.8
8	39.5
9.9	37.6

Table A.5 PSL transmission efficiency of XMX/2A using 1μm-9.9 μm AD PSL particles without dilution air

Particle size(μm)	Efficiency(%)
1	1.5
2	13.7
3	17.8
5	29
8	16.2
9.9	3.6

APPENDIX B

FIGURES

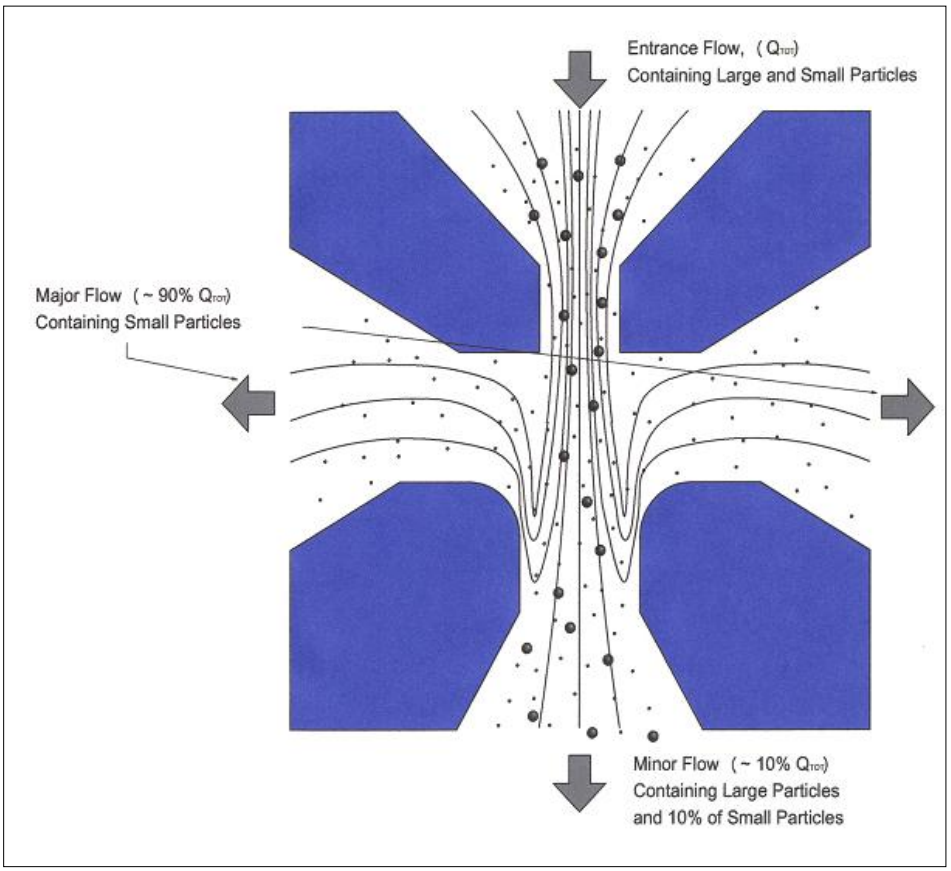

Figure B.1 Schematic of virtual impactor concept

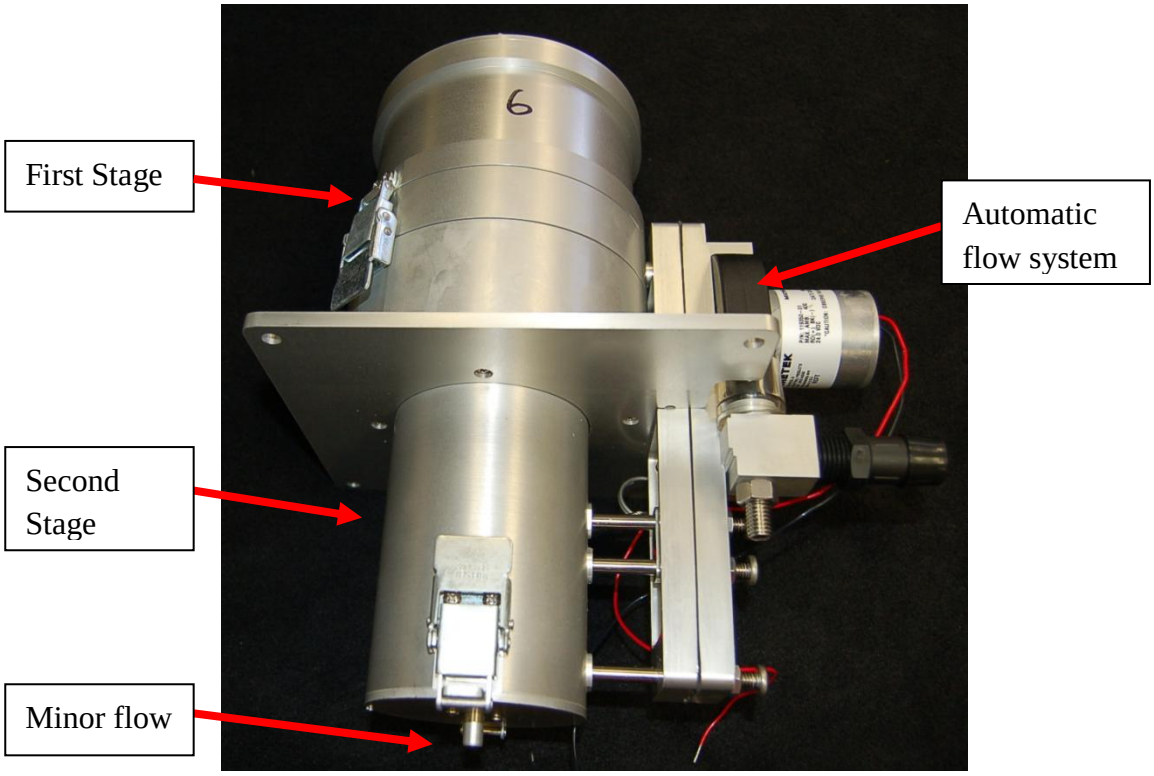

Figure B.2a Two-stage 100 L/min circumferential slot virtual impactor

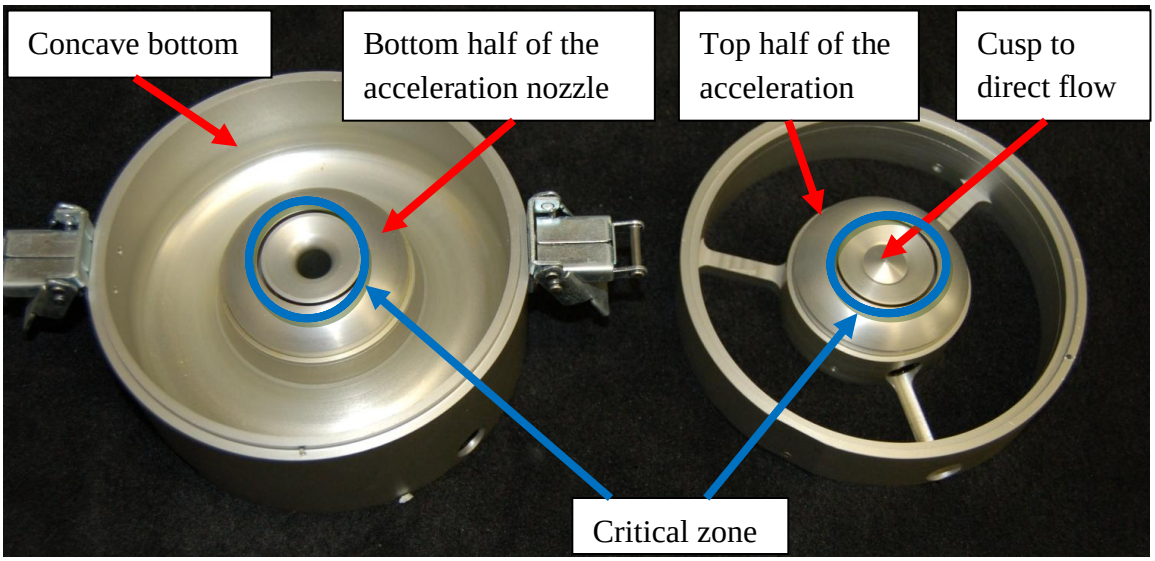

Figure B.2b First stage of two-stage 100 L/min circumferential slot virtual impactor

(LaCroix 2008)

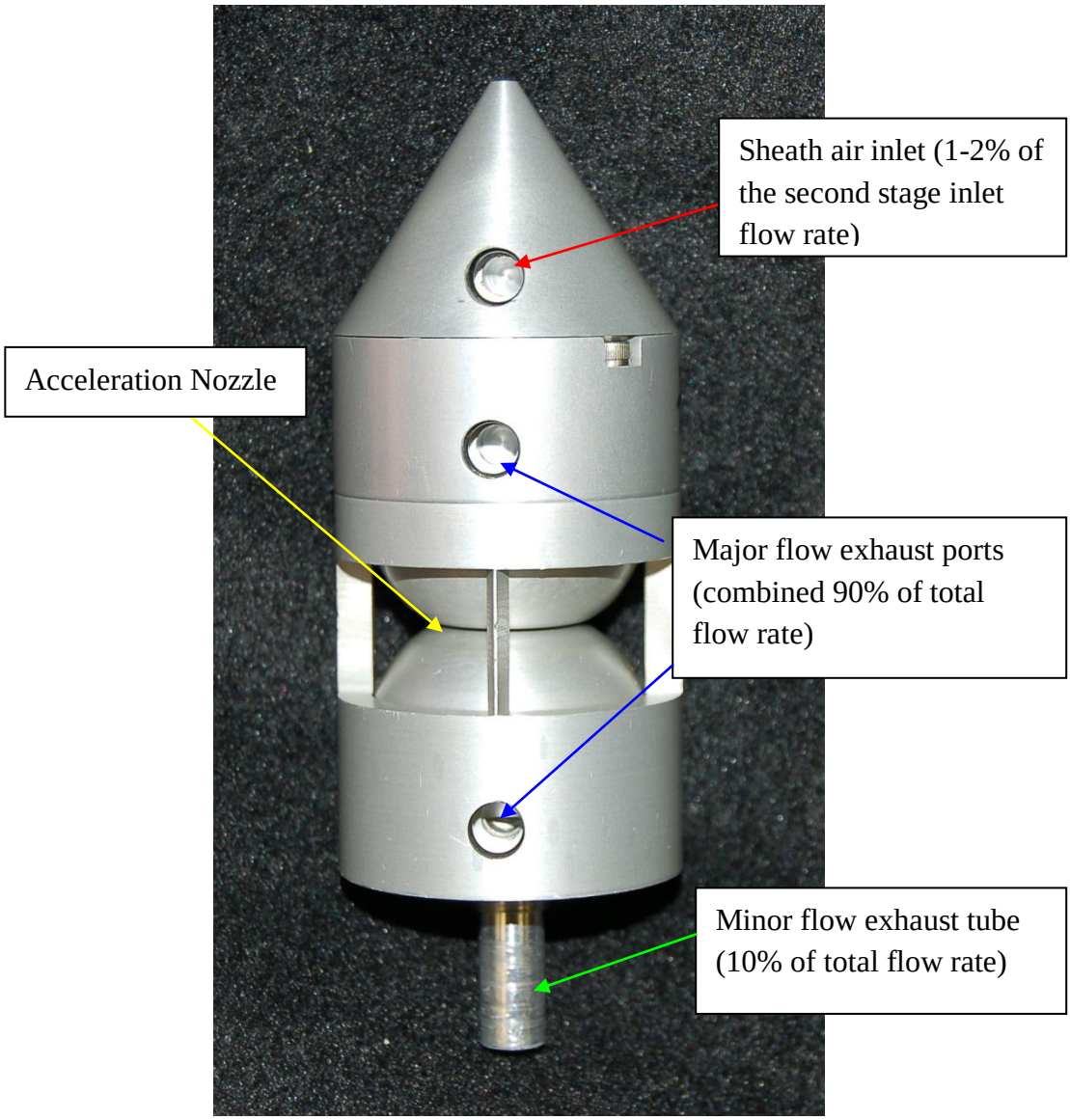

Figure B.2c Two-stage 100 L/min circumferential slot virtual impactor (LaCroix 2008)

Figure B.3 100 L/min in-line virtual impactor

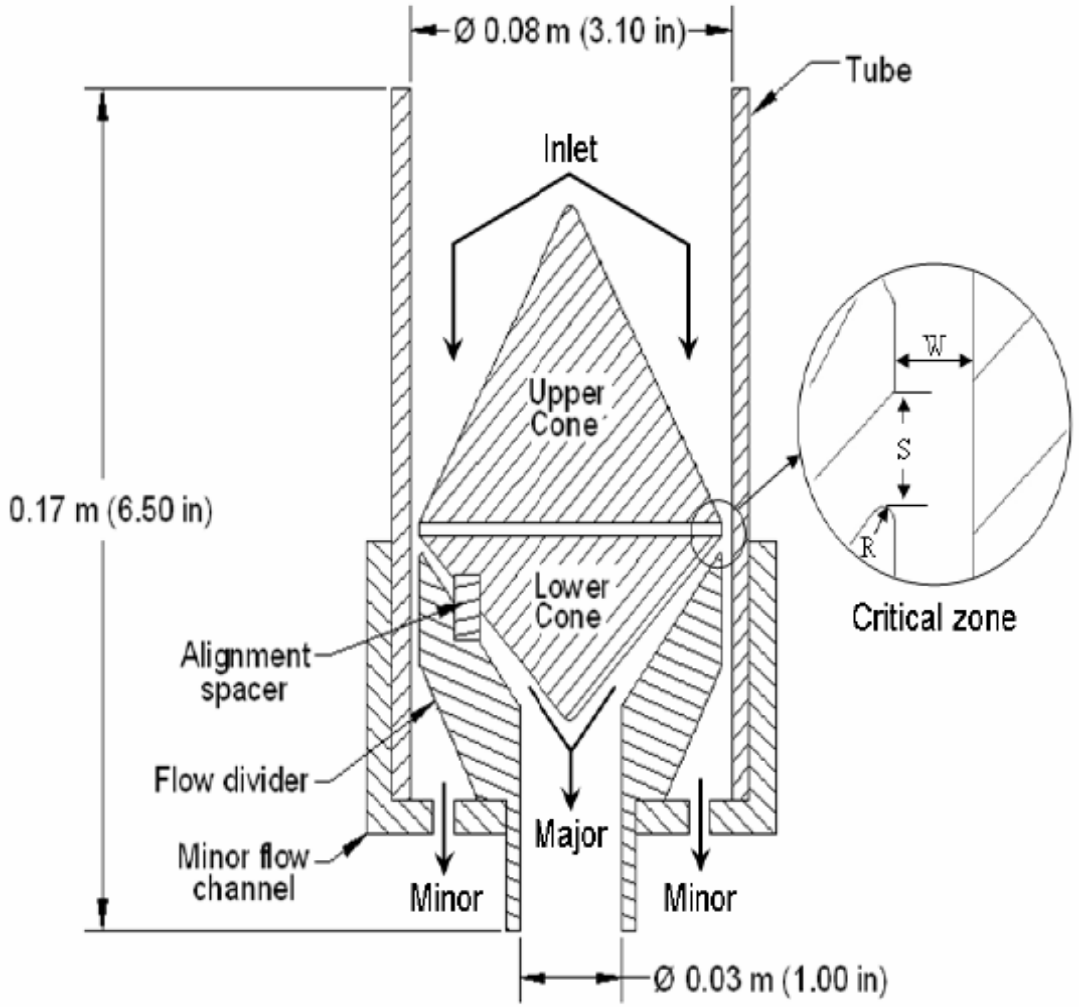

Figure B.4 Schematic of the in-line virtual impactor prototype (Seshadri 2007)

Figure B.5a Three-stage aerosol concentrator XMX/2A (Kesavan et al., 2008)

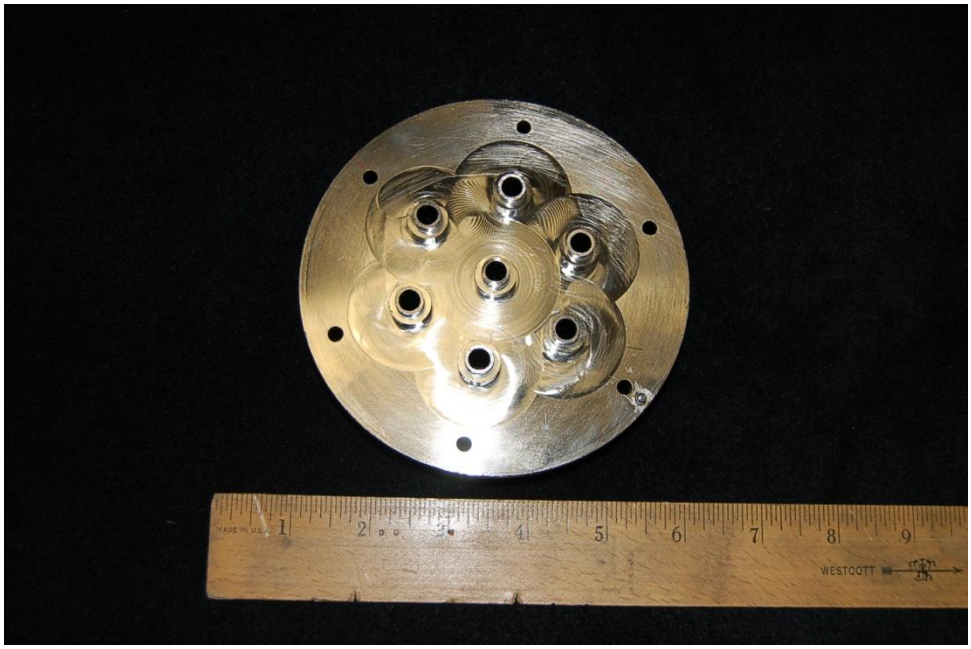

Figure B.5b First stage of aerosol concentrator XMX/2A

Figure B.5c Second stage of aerosol concentrator XMX/2A

Figure B.5d Third stage of aerosol concentrator XMX/2A

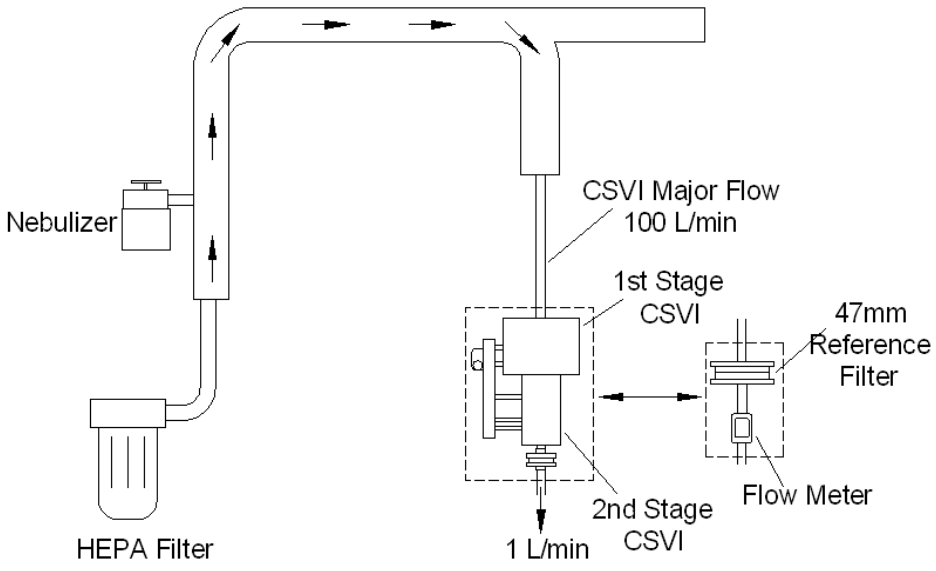

Figure B.6 Two-stage CSVI setup with nebulizer for PSL test

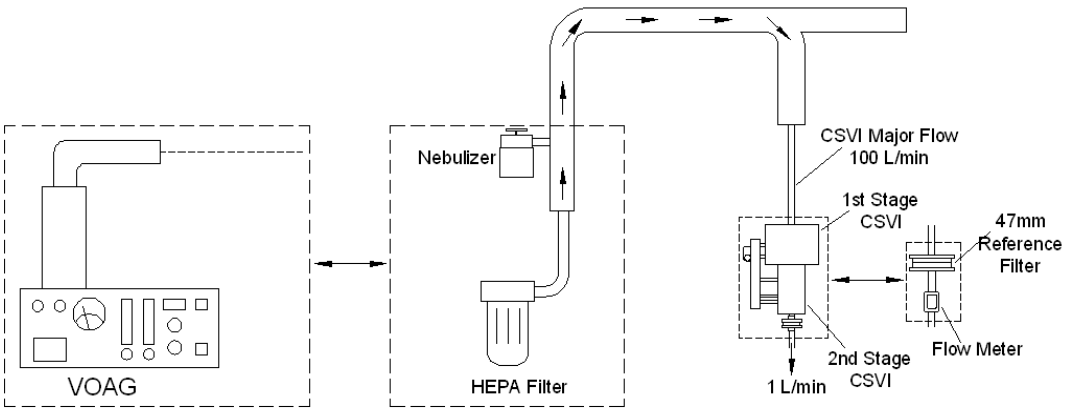

Figure B.7 Two-stage CSVI setup with VOAG for oleic acid test

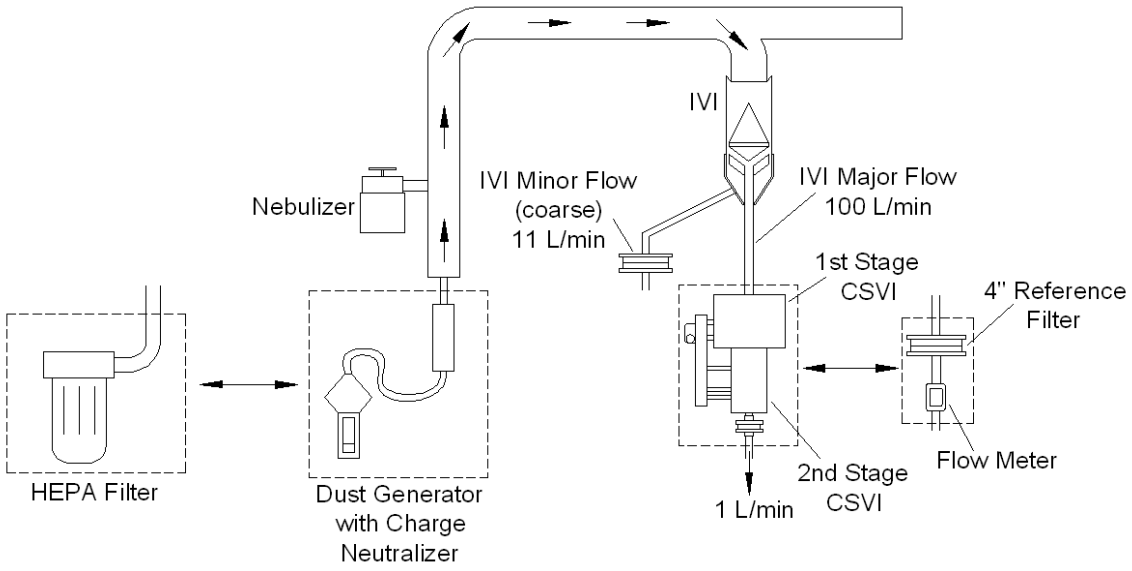

Figure B.8 Dust test setup

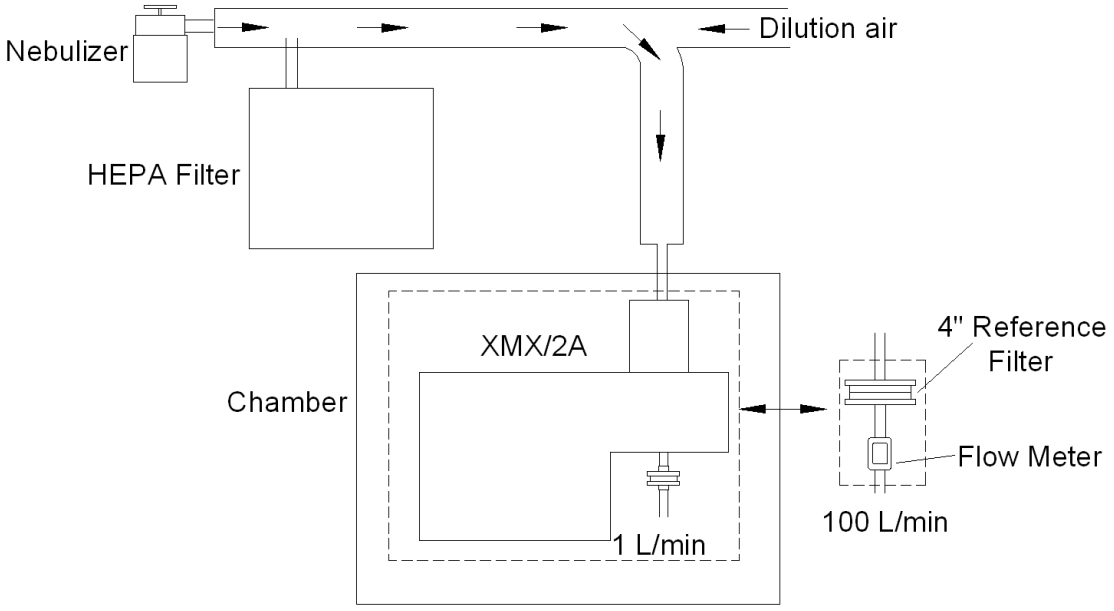

Figure B.9 XMX/2A setup with dilution air for PSL test

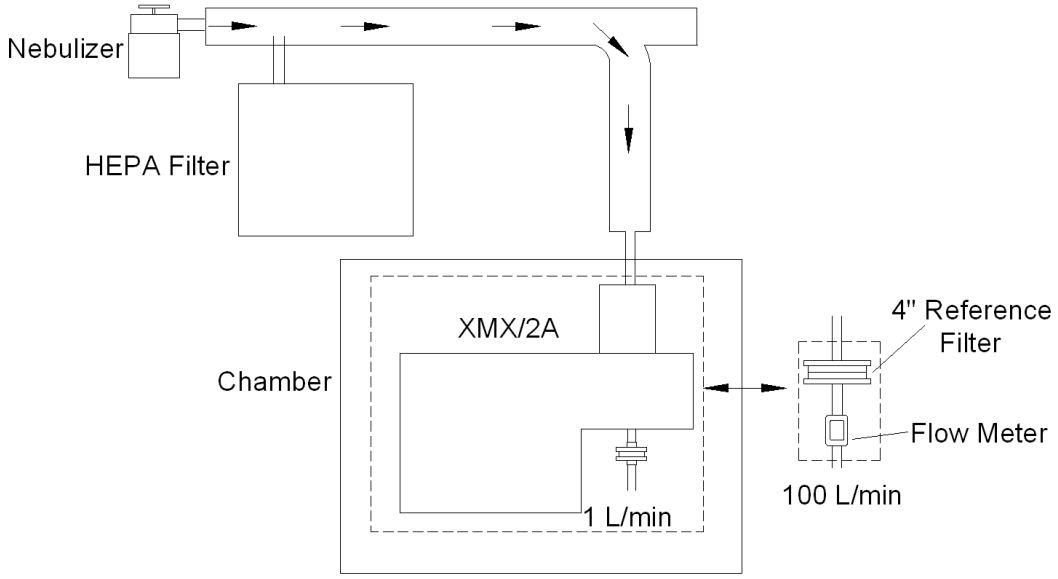

Figure B.10 XMX/2A setup without dilution air for PSL test

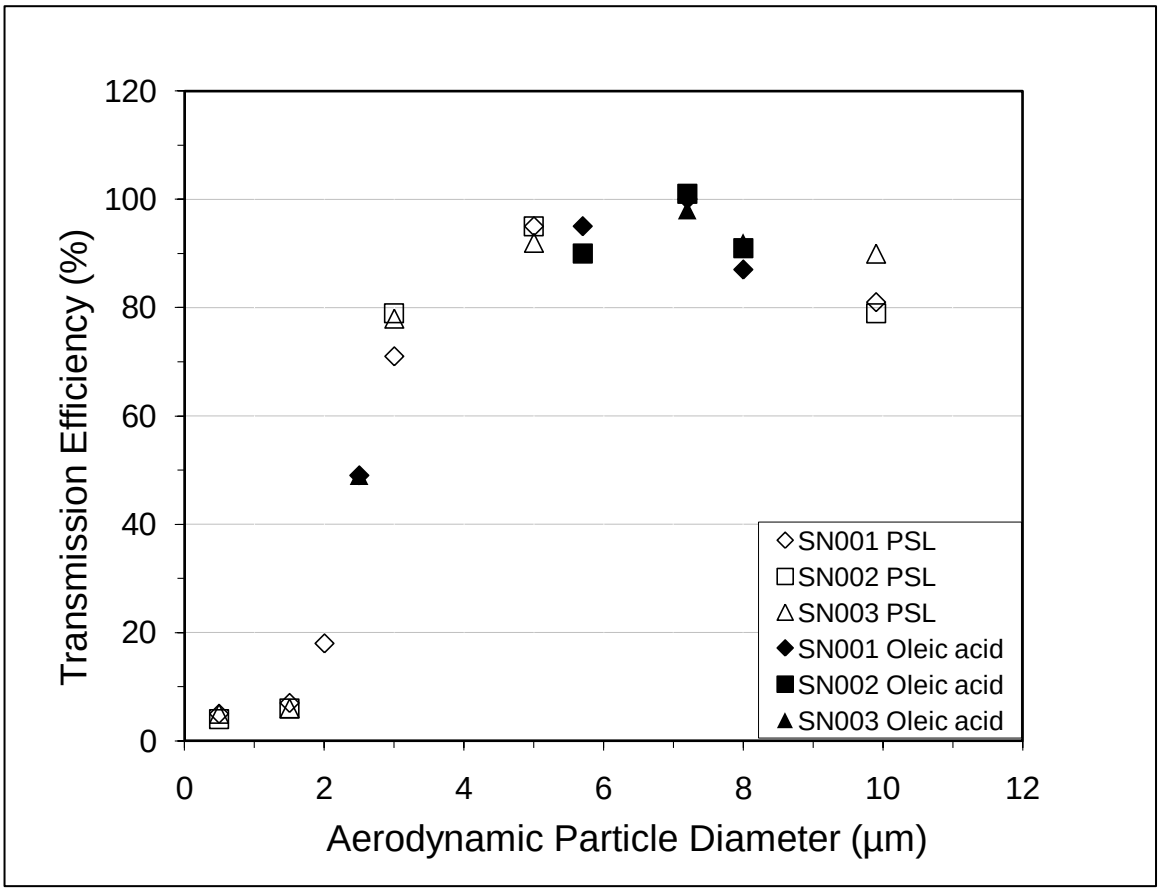

Figure B.11 Transmission efficiency of the three TSI two-stage 100 L/min units using PSL and oleic acid particles 0.49 µm-9.9 µm AD

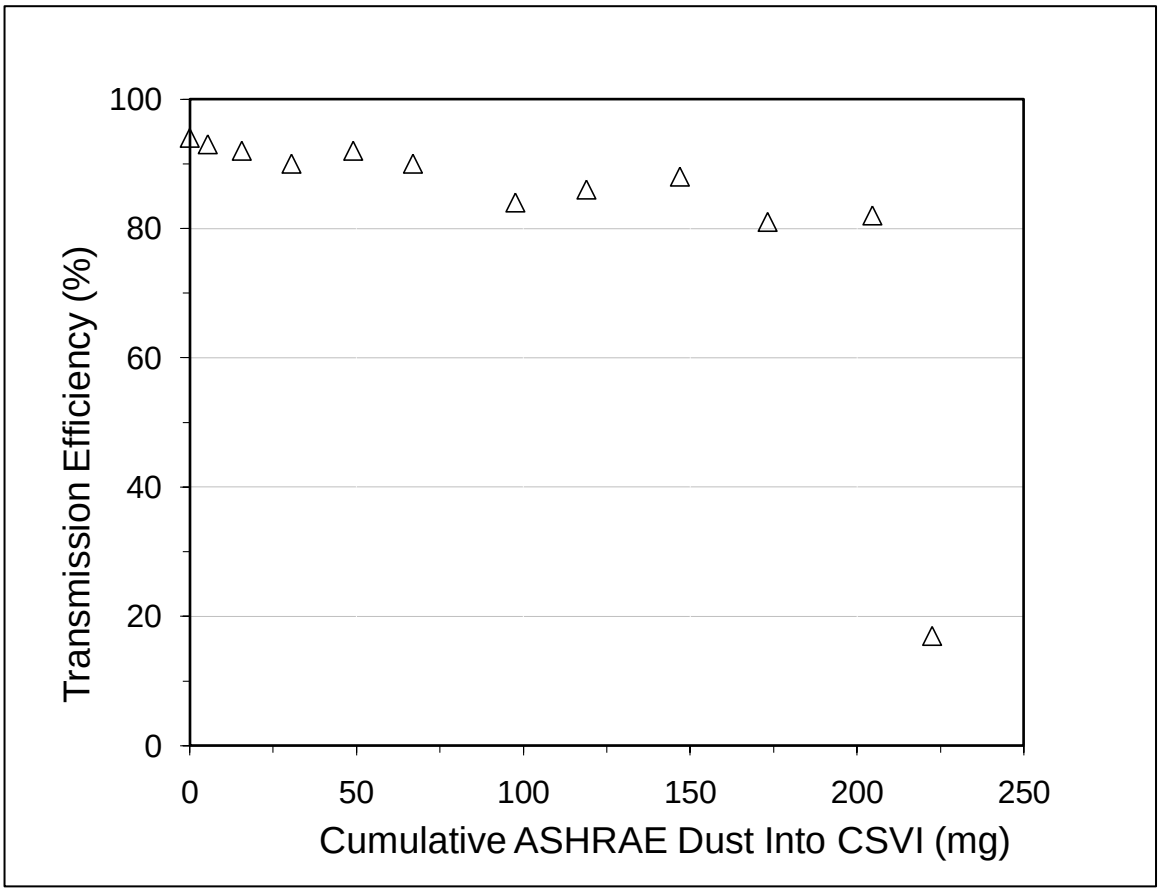

Figure B.12a PSL (5 μm) transmission efficiency of a two-stage 100 L/min CSVI (TSI SN/003) in the presence of increasing amounts of ASHRAE dust

Figure B.12b ASHRAE dust deposit in the CSVI SN003 unit after the experiment

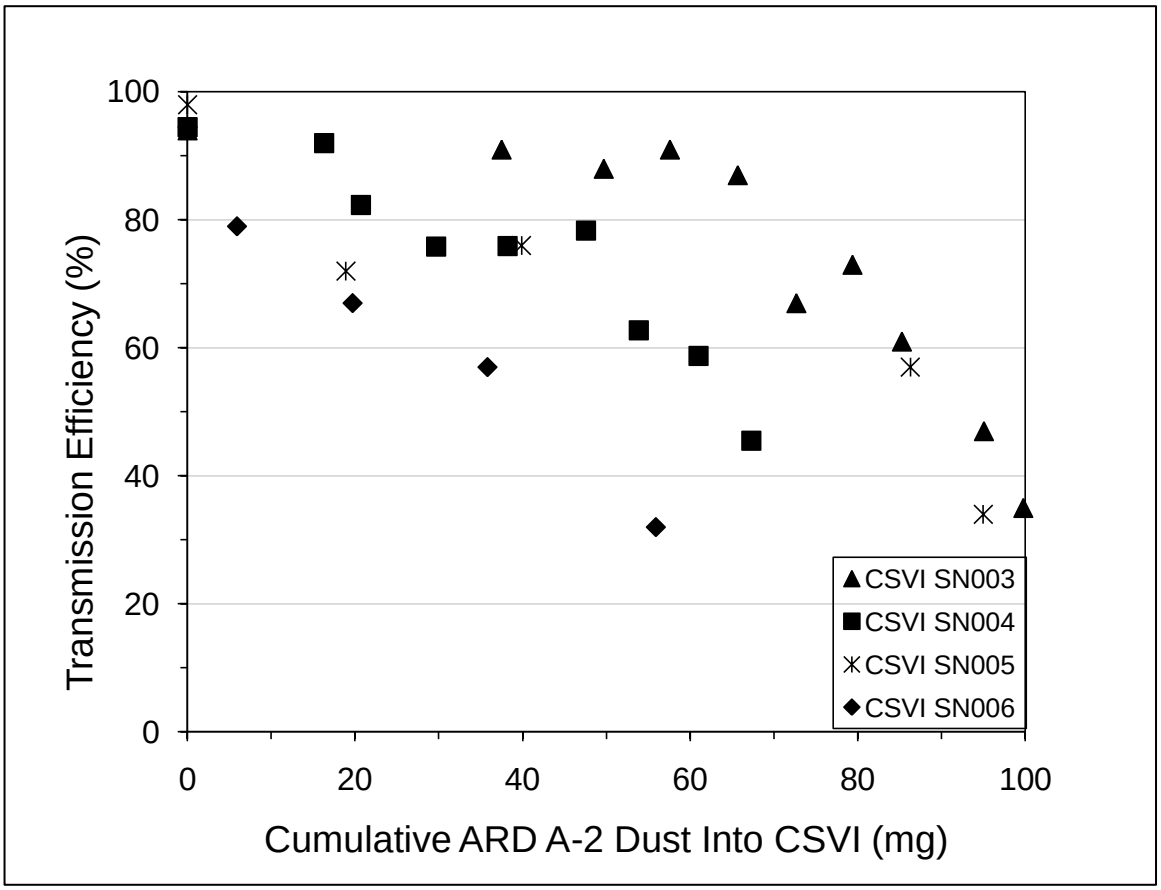

Figure B.13a PSL (5 μm) transmission efficiency of the IVI-CSVI SN003-006 in the presence of increasing amounts of ARD A-2 dust

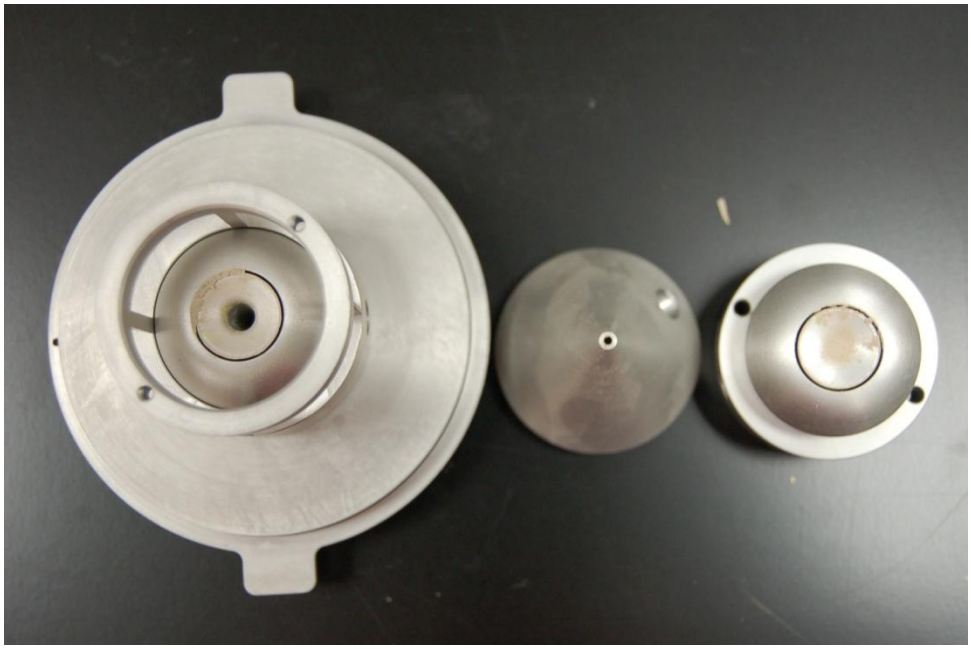

Figure B.13b ARD A-2 dust deposition in the CSVI SN003 unit after the experiment

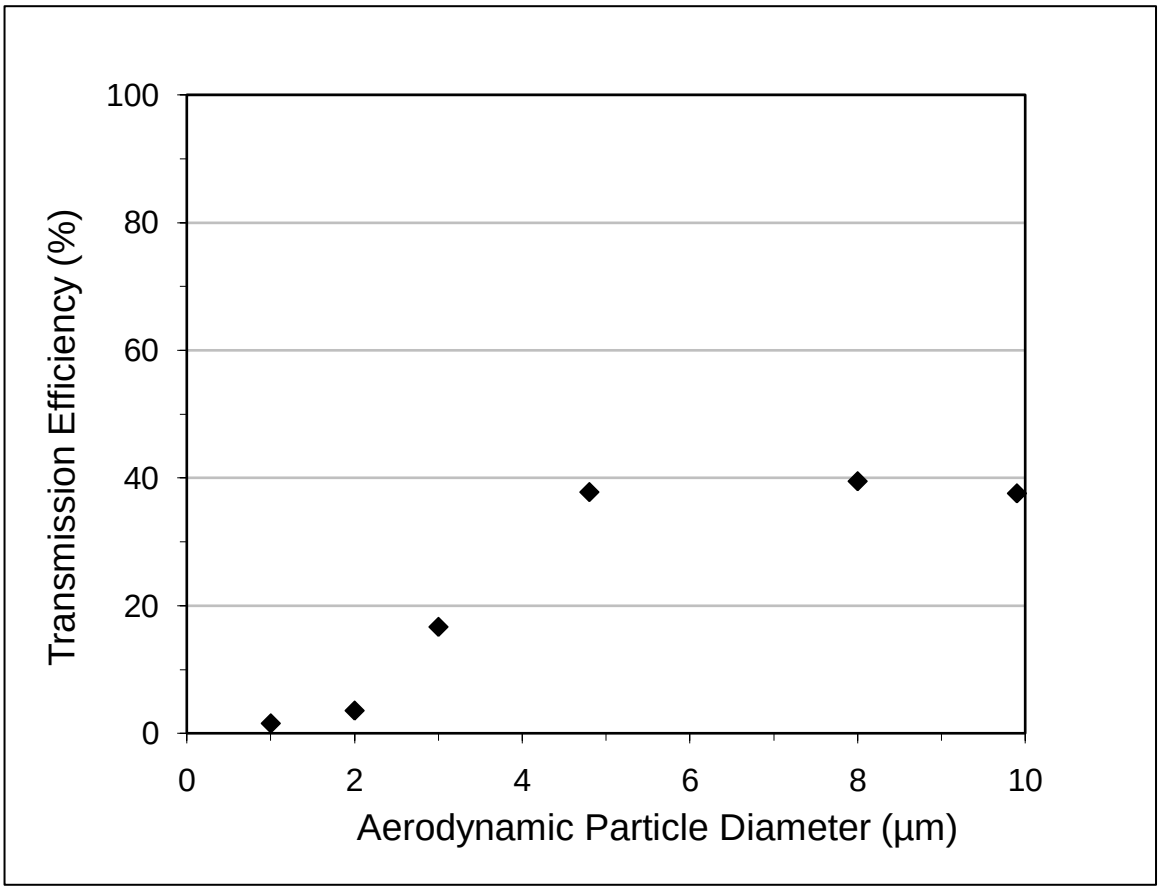

Figure B.14 PSL transmission efficiency of XMX/2A using 1µm-9.9 µm AD PSL particles with dilution air

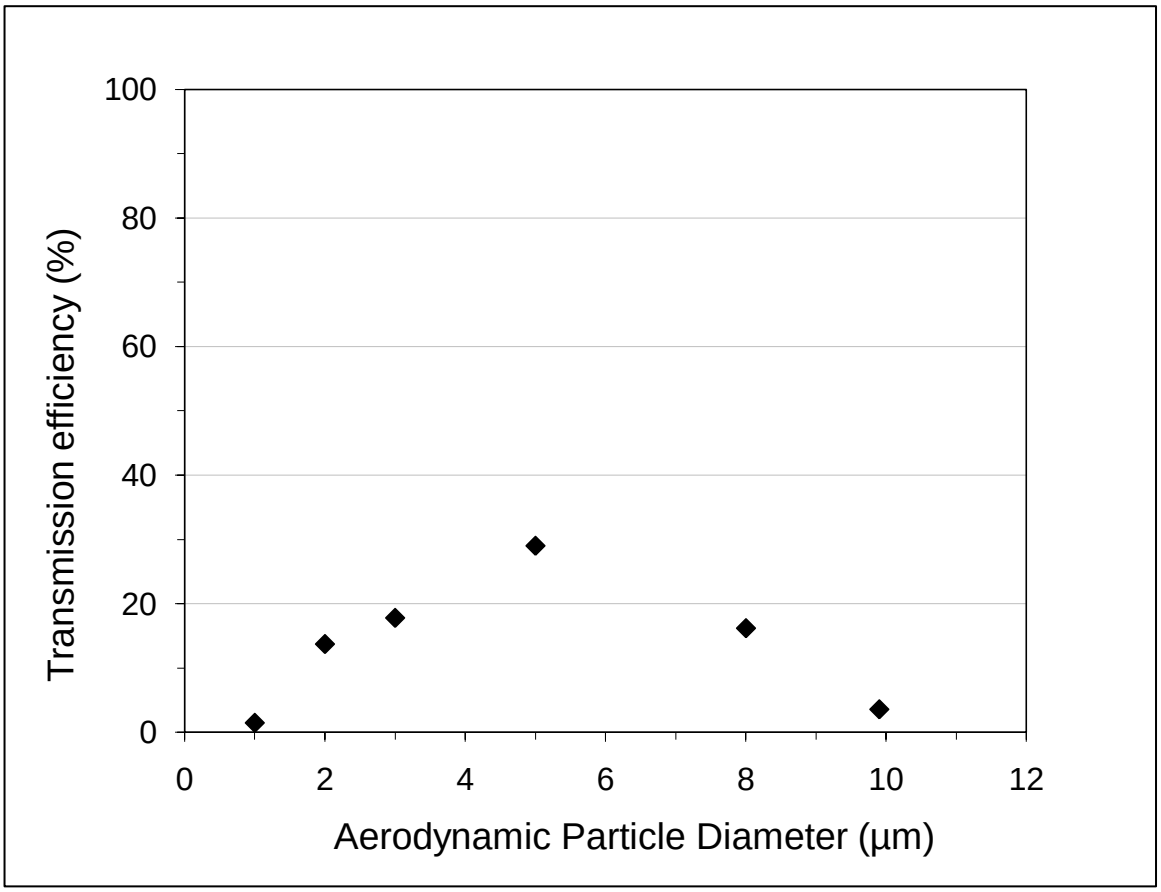

Figure B.15 PSL transmission efficiency of XMX/2A using 1µm-9.9 µm AD PSL particles without dilution air

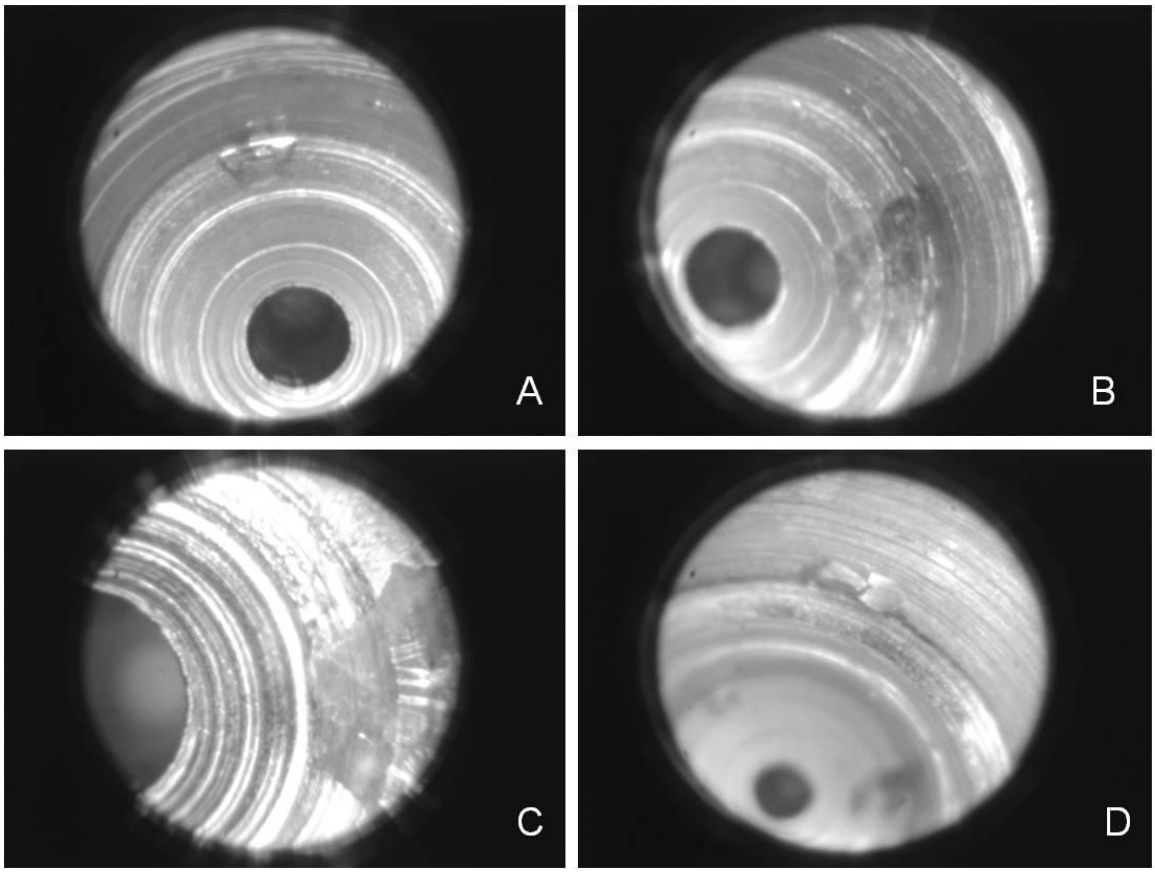

Figure B.16 Borescope images of discolored/damaged areas inside the XMX/2A second stage ¼" nozzle at the connection to the 1/20" section

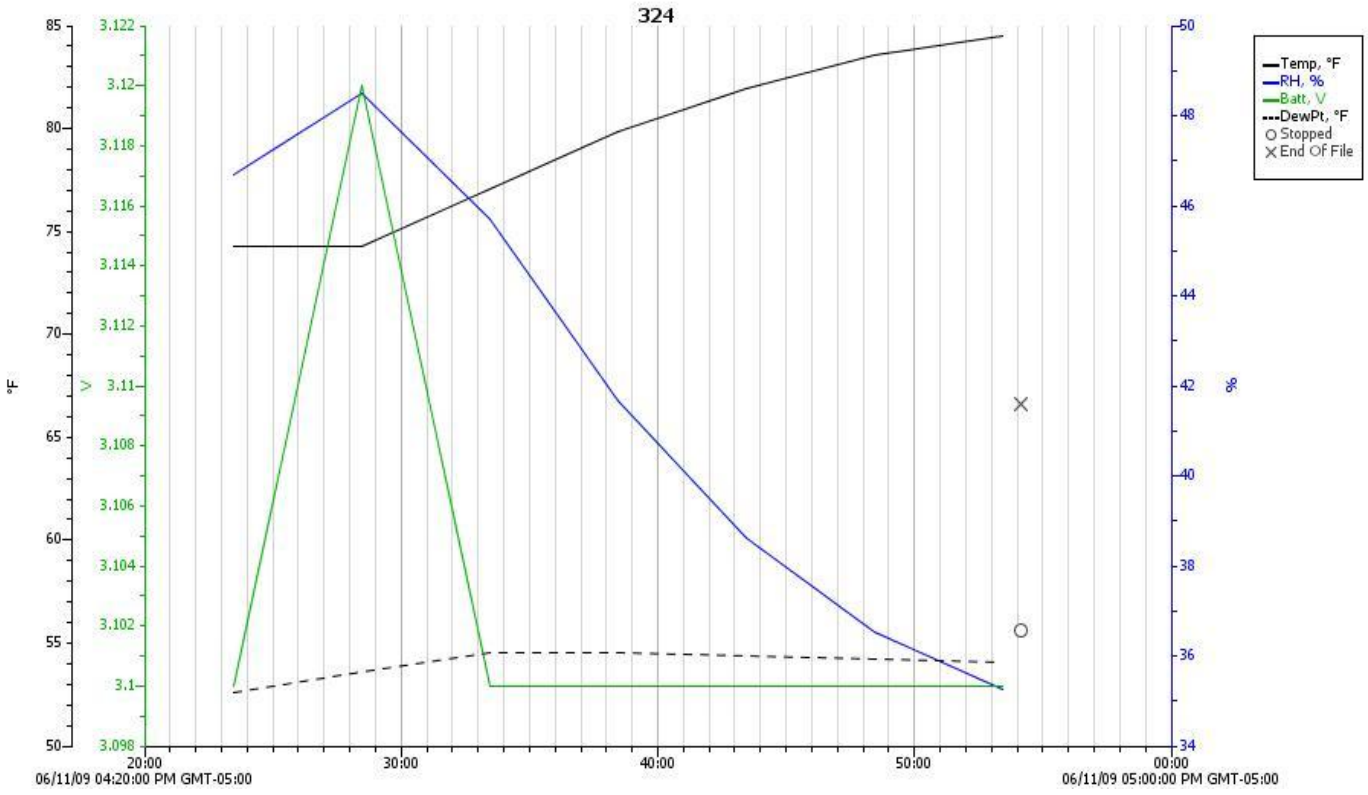

Figure B.17 Relative humidity (RH), temperature (temp), dew point (dewpt) and battery (batt) in the XMX/2A testing chamber during 30 minutes test at 100 L/min air flow. Atomization started at 04:23:50 PM and ended at 04:54:00 PM.

VITA

Name: Jing Wen

Address: Aerosol Technology Lab, Texas A&M University,
Mechanical Engineering Dept, TAMU 3123,
College Station, TX 77843-3123

Email Address: wenjane@neo.tamu.edu

Education: B.S., Thermal and Power Engineering, Xi'an Jiaotong University, China, 2007
M.S., Mechanical Engineering, Texas A&M University, 2009